Initial Research on Vibration Reduction for Quadcopter Attitude Control: An Additive-state-decomposition-based Dynamic Inversion Method

ZHANG Jing
School of Automation Science and Electrical Engineering
Beihang University
Beijing 100191, P.R.China
Email: zhangjing93@buaa.edu.cn

DU Guang-Xun
School of Automation Science and Electrical Engineering
Beihang University
Beijing 100191, P.R.China
Email: dgx@buaa.edu.cn

QUAN Quan
School of Automation Science and Electrical Engineering
Beihang University
Beijing 100191, P.R.China
Email: qq_buaa@buaa.edu.cn

***Abstract*—In practice, the lift that a propeller produces is composed of theoretical value and fluctuation, which results in vibration in aircraft. This paper will analyze the effect of the fluctuation on the quadcopter. In order to reduce the vibration caused by the fluctuation, an improved Additive-State-Decomposition-Based (ASDB) dynamic inversion stabilized controller is proposed. To show its effectiveness, the proposed controller is compared with the traditional ASDB dynamic inversion stabilized controller in numerical simulations. Simulation results show that a better damping performance for lift fluctuation is achieved with the improved ASDB dynamic inversion stabilized controller. Then the continuous-time controller is further discretized by Tustin transformation method with prewarping to be a digital controller in different sampling time, and the ideal sampling time is found out to trade off cost and performance of the digital controller.**

***Index Terms*—Quadcopter, vibration, lift fluctuation, additive state composition (ASD), Tustin transformation method, prewarping.**

I. Introduction

Vibration often exists in aircraft during flight [2]. There are a few different sources accounting for the vibration, all of which can be attributed to mechanical structure, aerodynamics, and external factors. For mechanical structure factors, the sources are mainly from frame deformation. Besides, any looseness can also contribute to vibration since most accessories are mounted on the aircraft. The source in mechanical structure can be greatly reduced by improving stiffness and installation. For aerodynamics factors, as the flow field around aircraft in flight is complicated, especially at high speed, there will be pressure unexpected produced because of the interaction of each part, which further acts on the aircraft, resulting in a vibration. As we know, for rotorcraft, the lift coefficient produced by propellers is derived for isolated propeller, while for the installed configuration, it may change with surrounding flow field. Aircraft can also undergo vibration in the presence of external factors such as atmospheric turbulence, which can lead to nonuniform flow field. It is worth noting that the sensor onboard can further amplify the effect of vibration, reflected in the input of controller. Then a signal containing vibration information will be delivered by the controller to actuators, finally causing a vibration.

For quadcopter, the lift and torque produced by propellers are proved to be proportional to the square of propeller angular velocity theoretically. Therefore, the lift and torque could be considered as a fixed value given a specified propeller speed. However, in practice, the actual lift of quadcopter is composed of a theoretical value and a series of high-frequency components related to the propeller angular velocity [2]. The high-frequency component can be regarded as lift fluctuation, which partly accounts for the vibration. Acting as an excitation force, lift fluctuation can be further transformed into torque, affect the attitude dynamics and finally cause a vibration. The vibration in quadcopter usually has bad effects. When vibration exists, some of the energy meant for propulsion is directed toward shaking the body. What is more, large-amplitude vibration will cause measurement noise in sensor measurements. Furthermore, vibration can result in fatigue breakage of related components. Thus, it is of great importance to consider the vibration resulted from lift fluctuation in design and control.

Currently, there have been a lot of research on the vibration reduction problem. All the research basically fall into three categories: reducing the excitation force in propellers, reducing the force transmitted to the body, and controlling or reducing the vibration in the body directly. Since propellers are the source of vibration, reducing the excitation force in propellers is preferred in vibration reduction methods, most of which in quadcopter are realized by ensuring static balance and dynamic balance [3], [4]. Besides, the technology that reduces the vibration transmitted to the body is applied to quadcopters using vibration absorber or isolation system. Meanwhile, in order to minimize the influence of vibration on the controller, a filter can be applied to the sensor [2]. With the development

978-1-5386-3524-7/17/$31.00 ©2017 IEEE

of the control theories, active control techniques for vibration reduction have made great progress, among which Active Control Structure Response (ACSR) is widely studied because of its effectiveness, adaptability, and easy-implementation [5]-[7]. The key idea of ACSR is to give a counter excitation force by actuators to eliminate vibration by detecting the response of body via sensors.

The methods introduced above reduce vibration but increase weight and cost. In order to overcome this drawback, an improved method based on the ASDB dynamic inversion stabilized control is proposed. The key idea behind the proposed method is to lump disturbance resulted from the lift fluctuation and other uncertainty into one disturbance by additive state decomposition, and then compensate for it in the lift by changing the angular velocity. Firstly, the dynamics of quadcopter attitude subject to lift fluctuation is formulated. Then, an improved ASDB dynamic inversion stabilized controller added by a band-pass filter is used to reject the disturbances. The designed continuous-time controller should be further discretized due to the fact that modern control systems are always implemented digitally [8]. There are several methods for the design of digital controllers [9]. Special attention is paid to the Tustin transformation method because of its ability to avoid frequency aliasing. In this paper, in order to make the digital controller to maintain the frequency characteristic in a critical frequency [10], the concept of prewarping is introduced to Tustin transformation. Besides the methods for controller discretization, the sampling period is also a critical factor that influences the performance of the digital controller. In order to perform like continuous-time controller, the sampling period is supposed to be sufficiently small [11]. While small sampling period means the increase of computation task. To achieve a relatively high level of control accuracy with a acceptable computation task, we should choose the sampling period that trades off these. Finally, the improved controller proposed in this paper is demonstrated in simulations to show the effectiveness compared with the original controller in [12]. Furthermore, the frequency characteristic of the digital controller based on continuous-time controller is obtained in different sampling period T_0, from which the suitable sampling period can be found out that trade off control accuracy and computation task.

The outline of this paper is developed as follows. In Section 2, we derive the mathematical statement of the problem, and system of quadcopter subject to vibration resulted from lift fluctuation is formulated as a control system under high-frequency disturbance. In Section 3, an improved ASDB dynamic inversion stabilized controller is used to reject the disturbance caused by the lift fluctuation, and the continuous controller is further discretized by Tustin transformation method with prewarping to a digital controller. Simulations are provided in Section 4. Finally in Section 5, concluding remarks are stated.

II. Problem Formulation

In this section, the mathematical model of the considered quadcopter subject to lift fluctuation is approached and formulated as a control system with high-frequency disturbance.

A. Quadcopter Model

The quadcopter is configured with four counter-rotating rotors symmetrically distributed around the center, which can be divided into two types, namely, the plus-configuration and X-configuration as shown in Fig.1. Here, the former is adopted. We use $S_I = \{\mathbf{e_x}, \mathbf{e_y}, \mathbf{e_z}\}$ to denote the Earth-Fixed Coordinate Frame (EFCF), and $S_b = \{\mathbf{e_1}, \mathbf{e_2}, \mathbf{e_3}\}$ to denote the Aircraft-Body Coordinate Frame (ABCF) as shown in Fig.1(a), where $\mathbf{e_3}$ grows downward according to the right-hand principle. On this basis, the attitude dynamical model is expressed.

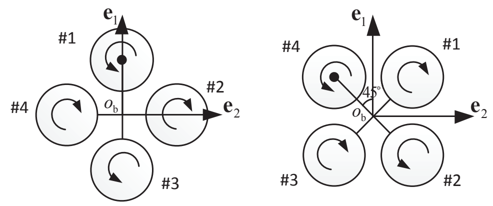

(a) Plus-configuration (b) X-configuration

Fig. 1. Quadcopters with two configurations

As shown in Fig.1, the lift f_i and counter torque M_i produced by propeller i can be expressed as

$$f_i = C_{\mathrm{T}} \varpi_i^2, M_i = C_{\mathrm{M}} \varpi_i^2 \tag{1}$$

where $C_{\mathrm{T}}, C_{\mathrm{M}} \in \mathbb{R}^+$ represent the thrust coefficient and the torque coefficient, respectively; $\varpi_i \in \mathbb{R}^+$ is the angular velocity of the propeller i. Then the mapping between the lift $\mathbf{f} = \begin{bmatrix} f_1 & f_2 & f_3 & f_4 \end{bmatrix}^{\mathrm{T}}$ and the total control $\mathbf{u} = \begin{bmatrix} F & \tau_x & \tau_y & \tau_z \end{bmatrix}^{\mathrm{T}}$ applied to the quadcopter can be further expressed as

$$\mathbf{u} = \mathbf{Hf} \tag{2}$$

where the nominal constant control input matrix

$$\mathbf{H} = \begin{bmatrix} 1 & 1 & 1 & 1 \\ 0 & -r & 0 & r \\ r & 0 & -r & 0 \\ \frac{C_{\mathrm{M}}}{C_{\mathrm{T}}} & -\frac{C_{\mathrm{M}}}{C_{\mathrm{T}}} & \frac{C_{\mathrm{M}}}{C_{\mathrm{T}}} & -\frac{C_{\mathrm{M}}}{C_{\mathrm{T}}} \end{bmatrix} \tag{3}$$

and r is the distance from the propeller center to the mass center of the quadcopter.

The linear attitude dynamical model around hover condition under the small-angle assumption [13] in the ABCF is established as

$$\mathbf{J} \cdot {}^{\mathrm{b}}\dot{\boldsymbol{\omega}} = \boldsymbol{\tau} \tag{4}$$

where $\boldsymbol{\tau} = \begin{bmatrix} \tau_x & \tau_y & \tau_z \end{bmatrix}^{\mathrm{T}} \in \mathbb{R}^3$ and ${}^{\mathrm{b}}\boldsymbol{\omega} = \begin{bmatrix} \omega_{x_b} & \omega_{y_b} & \omega_{z_b} \end{bmatrix}^{\mathrm{T}}$ are the moments generated by the propellers in the body axes and angular velocity of the aircraft body's rotation, respectively; $\mathbf{J} = \mathrm{diag}\{J_x, J_y, J_z\} \in \mathbb{R}^{3\times 3}$ represents the moments of inertia in the body axes.

B. The Effect of Lift Fluctuation on Attitude Dynamic

In [2], the lift is tested in time and frequency field, and the result indicates that the lift is a periodic signal, where the energy is mainly concentrated on fundamental frequency, which is consistant with the angular velocity of propeller. On this basis, the lift can be further expressed as follows:

$$f_i = \bar{f}_i + \sum_k A_i^k \sin(k\varpi_i t + \varphi_i^k) \tag{5}$$

where $\bar{f}_i = C_\mathrm{T}\varpi_i^2$ represents the theoretical value; A_i^k and φ_i^k represent the amplitude and phase angle of k-th harmonic, respectively; $\sum\limits_k A_i^k \sin(k\varpi_i t + \varphi_i^k)$ represents the component of lift fluctuation. Combining (3) and (5), the total force for the quadcopter can be expressed as

$$F = \sum_{i=1}^{4} f_i = \sum_{i=1}^{4} (\bar{f}_i + \sum_k A_i^k \sin(k\varpi_i t + \varphi_i^k)). \tag{6}$$

The total torque resulted from lift in practice for quadcopter can be expressed as

$$\begin{array}{l} \tau_x = (\bar{f}_4 - \bar{f}_2)r + \Delta\tau_x = \bar{\tau}_x + \Delta\tau_x \\ \tau_y = (\bar{f}_1 - \bar{f}_3)r + \Delta\tau_y = \bar{\tau}_y + \Delta\tau_y \end{array} \tag{7}$$

where

$$\begin{array}{l} \Delta\tau_x = r\sum\limits_k (A_4^k \sin(k\varpi_4 t + \varphi_4^k) - A_2^k \sin(k\varpi_2 t + \varphi_2^k)) \\ \Delta\tau_y = r\sum\limits_k (A_1^k \sin(k\varpi_1 t + \varphi_1^k) - A_3^k \sin(k\varpi_3 t + \varphi_3^k)) \end{array} \tag{8}$$

and the torque resulted from lift fluctuation can be regarded as the disturbance torque, namely, $\Delta\tau_x$ and $\Delta\tau_y$. Around the hover condition, the angular velocities for the propellers are almost equal, namely, all the propeller angular velocities can regarded as ϖ. Therefore the disturbance torque $\Delta\tau_x$ and $\Delta\tau_y$ can be rewritten as

$$\begin{array}{l} \Delta\tau_x = r\sum\limits_k (A_4^k \sin(k\varpi t + \varphi_4^k) - A_2^k \sin(k\varpi t + \varphi_2^k)) \\ \Delta\tau_y = r\sum\limits_k (A_1^k \sin(k\varpi t + \varphi_1^k) - A_3^k \sin(k\varpi t + \varphi_3^k)) \end{array} \tag{9}$$

The detailed linear attitude dynamical model of the quadcopter around hover condition can be rewritten as

$$\begin{array}{l} \dot{\mathbf{x}}_\phi = \mathbf{A}_0\mathbf{x}_\phi + \mathbf{b}(\bar{\tau}_x + \Delta\tau_x)/J_x \\ \dot{\mathbf{x}}_\theta = \mathbf{A}_0\mathbf{x}_\theta + \mathbf{b}(\bar{\tau}_y + \Delta\tau_y)/J_y \end{array} \tag{10}$$

where $\mathbf{x}_\phi = \left[\begin{array}{cc} \phi & \omega_{x_b} \end{array}\right]^\mathrm{T}$, $\mathbf{x}_\theta = \left[\begin{array}{cc} \theta & \omega_{y_b} \end{array}\right]^\mathrm{T}$, and

$$\mathbf{A}_0 = \left[\begin{array}{cc} 0 & 1 \\ 0 & 0 \end{array}\right], \mathbf{b} = \left[\begin{array}{c} 0 \\ 1 \end{array}\right]. \tag{11}$$

Note $\mathbf{x}_{\phi_\mathrm{c}} = \left[\begin{array}{cc} \phi_\mathrm{c} & 0 \end{array}\right]^\mathrm{T}$, $\mathbf{x}_{\theta_\mathrm{c}} = \left[\begin{array}{cc} \theta_\mathrm{c} & 0 \end{array}\right]^\mathrm{T}$ to be the control commands of system, where φ_c, θ_c are constant values. In order to transform the tracking problem (10) into a stabilizing problem, let

$$\mathbf{e}_\phi = \mathbf{x}_\phi - \mathbf{x}_{\phi_\mathrm{c}}, \mathbf{e}_\theta = \mathbf{x}_\theta - \mathbf{x}_{\theta_\mathrm{c}} \tag{12}$$

then

$$\mathbf{x}_\phi = \mathbf{e}_\phi + \mathbf{x}_{\phi_\mathrm{c}}, \mathbf{x}_\theta = \mathbf{e}_\theta + \mathbf{x}_{\theta_\mathrm{c}} \tag{13}$$

and

$$\begin{array}{l} \dot{\mathbf{e}}_\phi + \dot{\mathbf{x}}_{\phi_\mathrm{c}} = \mathbf{A}_0\mathbf{e}_\phi + \mathbf{A}_0\mathbf{x}_{\phi_\mathrm{c}} + \mathbf{b}(\bar{\tau}_x + \Delta\tau_x)/J_x \\ \dot{\mathbf{e}}_\theta + \dot{\mathbf{x}}_{\theta_\mathrm{c}} = \mathbf{A}_0\mathbf{e}_\theta + \mathbf{A}_0\mathbf{x}_{\theta_\mathrm{c}} + \mathbf{b}(\bar{\tau}_y + \Delta\tau_y)/J_y \end{array}. \tag{14}$$

By substituting (11) into (14), we have

$$\begin{array}{l} \dot{\mathbf{e}}_\phi = \mathbf{A}_0\mathbf{e}_\phi + \mathbf{b}(\bar{\tau}_x + \Delta\tau_x)/J_x \\ \dot{\mathbf{e}}_\theta = \mathbf{A}_0\mathbf{e}_\theta + \mathbf{b}(\bar{\tau}_y + \Delta\tau_y)/J_y \end{array} \tag{15}$$

which is a stabilizing problem. In practice, most disturbance can be regarded as low-frequency disturbance, which should be considered. We use the disturbances d_ϕ, d_θ to replace the low-frequency and lift fluctuation disturbances. The dynamics can be further reformulated as

$$\begin{array}{l} \dot{\mathbf{e}}_\phi = \mathbf{A}_0\mathbf{e}_\phi + \mathbf{b}(\bar{\tau}_x J_x^{-1} + d_\phi) \\ \dot{\mathbf{e}}_\theta = \mathbf{A}_0\mathbf{e}_\theta + \mathbf{b}(\bar{\tau}_y J_y^{-1} + d_\theta) \end{array}. \tag{16}$$

Considering the symmetry of quadcopter, here we only design the controller for ϕ channel, therefore the dynamics can be rewritten as

$$\dot{\mathbf{e}}_\phi = \mathbf{A}_0\mathbf{e}_\phi + \mathbf{b}(\bar{\tau}_x J_x^{-1} + d_\phi) \tag{17}$$

Remark 1. Since the lift only fluctuates in the direction of the $\mathbf{e_3}$, there will be additional moments $\Delta\tau_x, \Delta\tau_y$ produced, while no additional moment $\Delta\tau_z$ is produced. This means that the yaw channel cannot be affected by the lift fluctuation. Therefore, the dynamics of yaw channel is not considered in this paper.

C. Objective of the Paper

The control objective is to design a vibration-dampening controller u_ϕ to drive the attitude angle of quadcopter ϕ such that the attitude angle ϕ is uniformly ultimate boundedness by a small value as $t \to \infty$ in the presence of lift fluctuation and low-frequency disturbance.

III. Additive-State-Decomposition-Based Dynamic Inversion Stabilized Controller

A. ASDB Dynamic Inversion Stabilized Controller

The key idea of the ASD is represented in [12]. Then, the ASD theory is applied to the controller design of the system (17). It is easy to prove that $(\mathbf{A}_0,\mathbf{b})$ is controllable, so a matrix $\mathbf{k} = \left[\begin{array}{cc} k_1 & k_2 \end{array}\right]^\mathrm{T} \in \mathbb{R}^2$ can be found such that $\mathbf{A} = \mathbf{A}_0 - \mathbf{b}\mathbf{k}^\mathrm{T}$ is stable. Then design a controller as

$$\bar{\tau}_x = J_x(u_\phi - \mathbf{k}^\mathrm{T}\mathbf{e}_\phi). \tag{18}$$

Therefore the system (17) can be rewritten as

$$\dot{\mathbf{e}}_\phi = \mathbf{A}\mathbf{e}_\phi + \mathbf{b}(u_\phi + d_\phi) \tag{19}$$

where $\mathbf{A} = \mathbf{A}_0 - \mathbf{b}\mathbf{k}^\mathrm{T}$ and $\mathbf{e}_\phi(0) = \mathbf{e}_{\phi_0}$. Taking (19) as the original system, we choose the primary system as

$$\dot{\mathbf{e}}_{\phi_\mathrm{p}} = \mathbf{A}\mathbf{e}_{\phi_\mathrm{p}} + \mathbf{b}u_\phi, \mathbf{e}_{\phi_\mathrm{p}}(0) = 0 \tag{20}$$

and then by subtracting (20) from (19), the secondary system is obtained as

$$\dot{\mathbf{e}}_{\phi_\mathrm{s}} = \mathbf{A}\mathbf{e}_{\phi_\mathrm{s}} + \mathbf{b}d_\phi, \mathbf{e}_{\phi_\mathrm{s}}(0) = \mathbf{e}_{\phi_0}. \tag{21}$$

By the additive state decomposition, we have

$$\mathbf{e}_{\phi} = \mathbf{e}_{\phi_{\mathrm{p}}} + \mathbf{e}_{\phi_{\mathrm{s}}}. \tag{22}$$

According to the *Theorem 1* in [12], we define a new output $y = \mathbf{c}^{\mathrm{T}}\mathbf{e}_{\phi}$, then rearrange (20)-(22) to be

$$\begin{aligned} &\dot{\mathbf{e}}_{\phi_{\mathrm{p}}} = \mathbf{A}\mathbf{e}_{\phi_{\mathrm{p}}} + \mathbf{b}u_{\phi}, \mathbf{e}_{\phi_{\mathrm{p}}}(0) = 0 \\ &y = y_p + d_l \end{aligned} \tag{23}$$

where

$$d_l = y_s = \mathbf{c}^{\mathrm{T}}\mathbf{e}_{\phi_{\mathrm{s}}} = Gd_{\phi} \tag{24}$$

where d_l is called the lumped disturbance, and $G = \mathbf{c}^{\mathrm{T}}(s\mathbf{I}_2 - \mathbf{A})^{-1}\mathbf{b}$, $y_p = Gu_{\phi}$.

According to the design procedure in [12], we will design an ASDB dynamic inversion stabilized controller for (19) in four steps:

Step 1. Design a state feedback gain $\mathbf{k} \in \mathbb{R}^2$ as

$$\mathbf{k} = [\ 80 \quad 18\ ]^{\mathrm{T}} \tag{25}$$

which results in $\mathbf{A} = \mathbf{A}_0 - \mathbf{b}\mathbf{k}^{\mathrm{T}}$ with the two negative real eigenvalues $-8, -10$.

Step 2. Select eigenvector of $\mathbf{A}^{\mathrm{T}}$ corresponding to its eigenvalue -8 as

$$\mathbf{c} = [\ 10 \quad 1\ ]^{\mathrm{T}}. \tag{26}$$

Obviously, $\det(\mathbf{c}^{\mathrm{T}}\mathbf{b}) \neq 0$.

Step 3. From Step 1-Step 2, we have

$$G = \mathbf{c}^{\mathrm{T}}(s\mathbf{I}_2 - \mathbf{A})^{-1}\mathbf{b} = \frac{1}{s+8}. \tag{27}$$

As $\mathbf{e}_{\phi} = \mathbf{x}_{\phi} - \mathbf{x}_{\phi_{\mathrm{c}}}$, $\mathbf{x}_{\phi}$ is measurable and $\mathbf{x}_{\phi_{\mathrm{c}}}$ is known, therefore the output $y = \mathbf{c}^{\mathrm{T}}\mathbf{e}_{\phi}$ of the system (23) can be calculated. The output can also be rewritten to be

$$y = Gu_{\phi} + d_l. \tag{28}$$

Therefore the lumped disturbance d_l can be observed by

$$d_l = y - Gu_{\phi}. \tag{29}$$

For system (28), G is a known minimum-phase transfer function. In order to make $y = 0$, the dynamic inversion tracking controller u_{ϕ} is designed as

$$u_{\phi} = -G^{-1}Qd_l \tag{30}$$

where the filter $Q(s)$ is introduced to guarantee that the order of the denominator of $G^{-1}Q$ is not lower than that of its numerator. Substituting the controller (30) into (28) results in

$$y = (1 - Q(s))d_l. \tag{31}$$

Combining (24), output (31) can be further written as

$$y = G(1 - Q(s))d_{\phi}. \tag{32}$$

where d_{ϕ} is the disturbance including low-frequency signal and a series of high-frequency components related to the propeller angular velocity. From the spectrum analysis in [2], it can be seen that the energy is mainly distributed over the fundamental frequency. Moreover, the harmonic will be eliminated by vibration absorber on quadcopter. Therefore the series of high-frequency components in d_{ϕ} can be simplified to be a sinusoidal signal, whose frequency is same to the propeller angular velocity ϖ. In order to make $y = 0$, the filter $Q(s)$ is expected to reserve all the signal in d_{ϕ}, therefore the filter should be designed to be

$$Q = Q_1 + Q_2 = \frac{1}{\varepsilon s + 1} + \frac{(\omega_0/q)s}{s^2 + (\omega_0/q)s + \omega_0^2} \tag{33}$$

where Q_1 is a low-pass filter, used to pass the low-frequency signal in d_{ϕ}, while Q_2 is a band-pass filter, used to pass the signal whose frequency is around ω_0, which is defined as center frequency, and q is a quality factor, determining the bandwidth. Here, ω_0 is set to be ϖ.

Step 4. Choose appropriate parameters $\varepsilon > 0$ and q in practice to achieve a tradeoff between stabilizing performance and robustness.

From the ASDB dynamic inversion stabilized controller (31), we get the following roll angle controller for the quadcopter

$$u_{\phi} = -G^{-1}\left(\frac{1}{\varepsilon s + 1} + \frac{(\varpi/q)s}{s^2 + (\varpi/q)s + \varpi^2}\right)d_l. \tag{34}$$

Then the controller can be further written as

$$u_{\phi} = -G^{-1}Q(Gd_{\phi}) = -\,Qd_{\phi} \tag{35}$$

which implies that the performance of digital controller by discretization mainly depends on Q.

B. Design of Digital Controller by Tustin Transformation Method with Prewarping

In order to make the controller realizable by computer, the designed continuous-time controller should be discretized to a digital controller. In this paper, the Tustin transformation method with prewarping is selected due to its ability to avoid frequency aliasing and maintain the frequency characteristic at a critical frequency. In Tustin transformation method, the digital controller can be obtained by

$$D_z(z) = D(s)|_{s=\frac{2}{T}\frac{z-1}{z+1}} \tag{36}$$

where $D_z(z)$, $D(s)$ are digital controller and continuous-time controller, respectively. Then it has

$$\begin{aligned} j\omega_{\mathrm{A}} &= \tfrac{2}{T}\tfrac{e^{j\omega_{\mathrm{D}}T}-1}{e^{j\omega_{\mathrm{D}}T}+1} = \tfrac{2}{T}\tfrac{e^{j\omega_{\mathrm{D}}T/2}-e^{-j\omega_{\mathrm{D}}T/2}}{e^{j\omega_{\mathrm{D}}T/2}+e^{-j\omega_{\mathrm{D}}T/2}} \\ &= \tfrac{2}{T}\tfrac{2j\sin(\omega_{\mathrm{D}}T/2)}{2\cos(\omega_{\mathrm{D}}T/2)} = j\tfrac{2}{T}\tan\tfrac{\omega_{\mathrm{D}}T}{2} \end{aligned} \tag{37}$$

namely

$$\omega_{\mathrm{A}} = \frac{2}{T}\tan\frac{\omega_{\mathrm{D}}T}{2} \tag{38}$$

where $\omega_{\mathrm{A}}, \omega_{\mathrm{D}}$ are frequencies in s domain and z domain, respectively. The correspondence of frequency implies that there is frequency distortion after discretization, as shown in Fig.2

Considering the frequency distortion, the concept of prewarping is introduced to ensure $D_z(\mathrm{e}^{\mathrm{j}\varpi T}) = D(j\varpi)$. Therefore a factor is introduced for prewarping based on equation (38) as

$$\frac{\varpi}{\omega_{\mathrm{A}}} = \frac{\varpi}{\frac{2}{T}\tan\frac{\varpi T}{2}}. \tag{39}$$

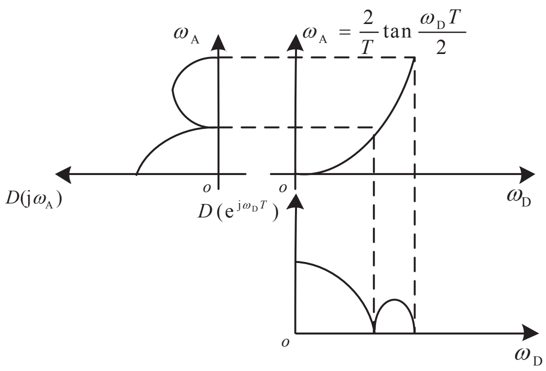

Fig. 2. Frequency distortions in Tustin transformation

Then the Tustin transformation with prewarping after improvement can be written as

$$D_z(z) = D(s)|_{s=\frac{\varpi}{\tan(\varpi T/2)}\frac{z-1}{z+1}}. \tag{40}$$

The closed-loop system in this paper with digital controller is shown in Fig.3, the part framed is completed in computer, which is digital.

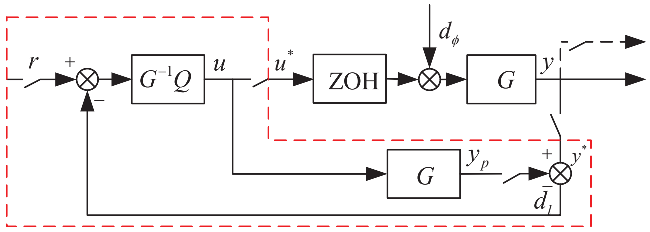

Fig. 3. Closed-loop system with digital controller

IV. Simulation

To demonstrate the effectiveness of the proposed controller for the quadcopter under lift fluctuation, simulations for the attitude control of quadcopter are carried out. The controller with low-pass filter is used to compare with the improved controller added by band-pass filter. Then, the controller is further discretized to be a digital controller based on the Tustin transformation with prewarping. The performance of digital controller depends highly on the sampling period T_0. Therefore the frequency characteristics of digital and continuous-time controller are displayed in different sampling period to find out the suitable value.

A. Simulation Parameter

In the simulation, the controller is designed for the propellers of quadcopter working around the angular velocity ϖ of $500rad/s$, and the four propellers are assumed to be in the same angular velocity. Here, the parameters for controller are chosen as: $\varepsilon = 1$, $\omega_0 = 500rad/s$, $q = 100$, and the moment of inertial $J_x = 0.02kg \cdot m^2$. In the simulation, the low-frequency disturbance is chosen to be a constant with magnitude of 0.2, and the lift fluctuation is set to be a sinusoidal factor $A\sin\varpi t$, where A is set to be 0.1. Here, the dynamics of propeller is considered and modeled by

$$\lambda_i = \frac{1}{t_p s+1} f_i, i \in \{1,2,3,4\} \tag{41}$$

where λ_i is the actual lift of propeller i, and the dynamic response parameter $t_p = 0.01$. In the original controller in [12], $Q = Q_1$, and in the improved controller proposed in this paper, $Q = Q_1 + Q_2$. The spectral analyses for the output of quadcopter with the two controllers at $\varpi = 500rad/s$ and $470rad/s$ are displayed in Fig.4-Fig.5, respectively.

With the chosen parameters, the transfer function $G_0(s)$ from d_l to y is obtained as

$$G_0(s) = 1 - Q = 1 - (\frac{1}{s+1} + \frac{5s}{s^2+5s+250000}). \tag{42}$$

To keep the frequency characteristic unchanged at $\varpi = 500rad/s$, the maximum sampling period T_m should be

$$T_m = 2\pi/2\varpi \approx 0.006s \tag{43}$$

according to Shannon sampling theorem. Therefore the sampling period T_0 can be chosen as $0.006, 0.004, 0.002, 0.001$. By discretization, it has

$$G_{0_{z1}}(z) = 1 - (\tfrac{1}{s+1} + \tfrac{12s}{s^2+12s+14400})\Big|_{s=\frac{z-1}{z+1}}$$
$$G_{0_{z2}}(z) = 1 - (\tfrac{1}{s+1} + \tfrac{12s}{s^2+12s+14400})\Big|_{s=\frac{\varpi}{\tan(\varpi T_0/2)}\frac{z-1}{z+1}}$$

where $G_{0_{z1}}(z)$, $G_{0_{z2}}(z)$ are digital transfer function by discretization, and the latter adds prewarping in the basis of Tustin transformation method, by which the effect of discretization in different sampling period time and the frequency characteristic of system can all be obtained. The amplitude-frequency characteristic of digital and continuous-time controllers in different sampling period T_0 is displayed in Fig.6.

B. Simulation Results

In Fig.4, it can be obviously seen that the frequency $f = 500/2\pi \approx 80Hz$ in spectral analysis of output is greatly reduced by the improved controller compared with original controller, which means the vibration is dampened. Therefore the improved controller outperforms the original controller in terms of vibration reduction in the presence of lift fluctuation. While in Fig.5, with other parameters unchanged and propeller angular velocity ϖ deviated from the center frequency of the designed band-pass filter, the high-frequency part in output can not be dampened effectively, therefore the performance of improved controller get poorer reflected in the spectral analysis of output.

The results in Fig.6 imply that the amplitude-frequency characteristic of digital controller based on Tustin transformation method with prewarping is almost consistent with that of continuous-time controller when $T_0 \leq 0.002$s, while the digital controller without prewarping requires a shorter sampling period T_0 to achieve the same performance. It can be seen that when $T_0 = 0.001$, the minimum sampling period that can be reached at present, the amplitude-frequency characteristic

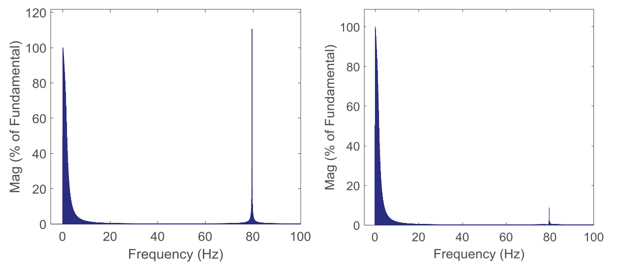

(a) Frequency characteristic of output with original controller (b) Frequency characteristic of output with improved controller

Fig. 4. Spectrum analysis of output when $\varpi = 500rad/s$

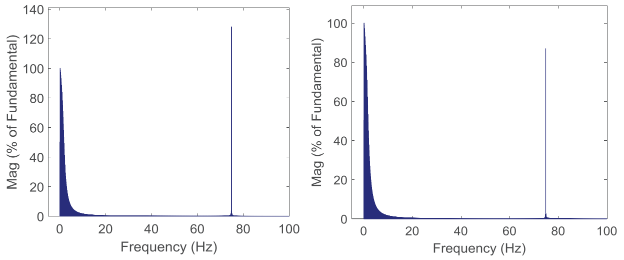

(a) Frequency characteristic of output with original controller (b) Frequency characteristic of output with improved controller

Fig. 5. Spectrum analysis of output when $\varpi = 470rad/s$

without prewarping cannot achieve a desired performance. It is of great superiority to prewarp in discretization to reduce sampling frequency, and further improve performance.

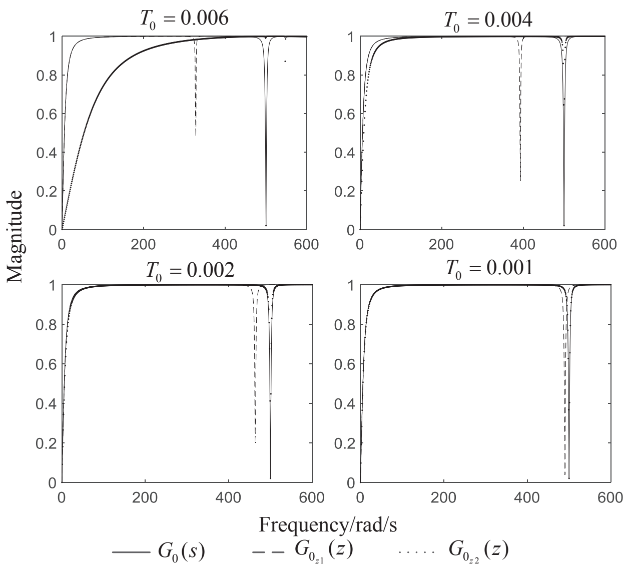

Fig. 6. Amplitude-frequency characteristic of digital and continuous-time controller in different sampling period

V. Conclusion

In this paper, the vibration reduction problem for quadcopter attitude control is studied. The main contributions of this paper are that: 1) the vibration reduction problem for quadcopter is formulated as a control problem subject to a high-frequency disturbance, and 2) an improved ASDB dynamic inversion stabilized control method added by a band-pass filter is used to reject the vibration regardless its amplitude; 3) the influence of prewarping on the frequency characteristic is shown, and it is proved that prewarping allows the sampling period to be shortened to achieve the same performance for the controller in this paper. The simulation results show that when the propeller works in the designed frequency, a good damping performance for lift fluctuation is achieved, while when the propeller angular velocity deviates from the designed value, the performance will be poor. Although the controller is designed for a specified propeller angular velocity, in most cases, the quadcopter works in hover and small-angle state, therefore, the precondition for the controller to be applied can be met.

VI. Acknowledgment

The financial supports from the National Natural Science Foundation of China (61473012) for this work are greatly acknowledged.

References

[1] Q. Quan, *Introduction to Multicopter Design and Control*, Singapore: Springer Press, 2017.
[2] C.-J Zhao, X. Gong, Y. Bai, "Interference and inhibition of lift fluctuation on quadcopter aircraft," *Optics and Precision Engineering,* vol. 22, no. 9, pp. 2431-2437, 2014.
[3] M. MacCamhaoil, Static and dynamic balancing of rigid rotors, *Bruel & Kjaer application notes*, BO, 0276-12.
[4] C. Wijerathne. (2016) Propeller balancing. [Online]. Available: http://okigihan.blogspot.com/p/propellerbalancing-propeller-unbalance.html.
[5] C.P. Kuo, R. Bruno, "Optimal actuator placement on an active reflector using a modified simulated annealing algorithm," in *Joint US/Japan Conf. on Adaptive Structures,* 1991, pp. 1056-1067.
[6] K.H. Baek, S.J. Euiott, "Natural algorithms for choosing source locations inactive control systems," *J Sound Vib,* vol. 186, no. 2, pp. 245-267, 1995.
[7] W. Gawronski, "Actuator and sensor placement for structural testing and control," *J Sound Vib,* vol. 208, no. 1, pp. 101-109, 1997.
[8] K.J. Åström, B. Wittenmark, *Computer-controlled Systems: Theory and Design*, Courier Corporation, 2013.
[9] J.-Y Gao, J. Xia, *Computer Control System,* Beijing: Tsinghua University Press, 2007.
[10] X.-B Sun, Y.-P Wang, Q. Zhou, "Research to the influence of prewarping on the design of filter," *System Engineering and Electronics,* vol. 29, no. 12, pp. 2032-2033, 2007.
[11] A.R. Teel, D. Nesic, P.V. Kokotovic, "A note on input-to-state stability of sampled-data nonlinear systems," in *Proc. 37th IEEE Conf. Decision and Control,* 1998, pp. 2473-2478.
[12] Q. Quan, G.-X Du, K.-Y Cai, "Proportional-integral stabilizing control of a class of MIMO systems subject to nonparametric cncertainties by additive-state-decomposition dynamic inversion design," *IEEE/ASME Trans. on Mechatronics,* vol. 21, no. 2, pp. 1092-1101, 2016.
[13] G.-X Du, Q. Quan, B. Yang, et al, "Controllability analysis for multirotor helicopter rotor degradation and failure," *Journal of Guidance, Control, and Dynamics,* vol. 38, no. 5, pp. 978-985, 2015.